# 3

Computational Industrial Mechanics

Highlights

- Checking the Variational Correctness of the Finite element Formulations through "Sweep test"
- Identification of the three Frequency Spectra (the axial, flexural and the shear) in a Curved Beam
- Implementation of Edge-Consistent QUAD4 Plate Bending Finite element in FINEART
- Validation and Verification of the Various Finite Elements Available in FINEART
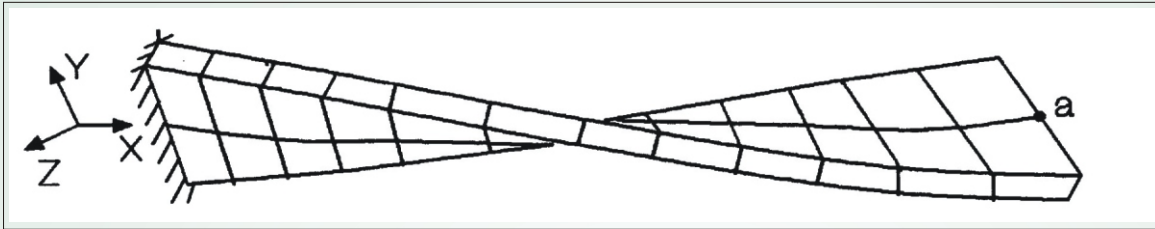
The Twisted Cantilever Benchmark Test

Inside

- Variational Correctness and Timoshenko beam Finite element Elastodynamics
- Free Vibration Analysis of Curved Beams
- Analysis of a Hybrid Beam Element with Timoshenko Stiffness and Classical Mass
- *A priori* error analysis of QUAD4 Element in Elastodynamic Problems
- Analysis of Mindlin Plate Element from the Function Space Approach
- Free Vibration Analysis of Composit Beams using Higher Orders Assure Deformation Theory
- The Motion of Periodically Forced Spheroids in Simple Shear Flow
- Isotropic Numerical Schemes
- The Quasi-Equilibrium Phase in Purely Nonlinear Chains with Boundaries

2005 Perspectives

- The new elements implemented in FINEART, will be benchmarked as per the standard tests

3.1 Variational correctness and Timoshenko beam finite element elastodynamics

The Timoshenko beam theory has features that make it an interesting case study for the examination of errors that appear when a finite element discretisation of its elastodynamics is made. Unlike the classical (or engineering) theory of beams, the Timoshenko theory incorporates shear flexibility and rotary inertia. As a consequence, it shows two distinct spectra, a basic flexural (or bending) dominated spectrum, and a shear dominated spectrum (Fig 3.1). Also, in the case of low order formulations (e.g. a two noded element), there is the possibility of locking, which has to be relieved using an extra-variational step such as reduced integration. Here, the error analysis implications for the two spectra, and that due to the extra-variational nature of reduced integration have been investigated.
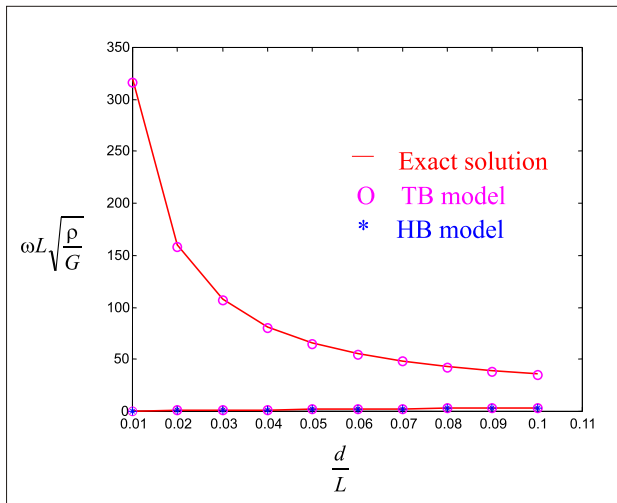

Fig 3.1 Dispersion diagram for the hinged-hinged Timoshenko beam for 3rd mode- Comparison of Timoshenko Beam and Hybrid Beam finite element model with the exact.

The boundedness aspect of the variationally correct finite element solution can be very elegantly demonstrated using a two element moving node sweep test for a one-dimensional problem. Fig 3.2 shows that the mid node can be located anywhere along the length. Each such configuration gives one possible global test function from the function space. The global stiffness and mass matrices are now a function of the node location. Each case would then give a Rayleigh- Ritz solution to the eigenvalue problem.
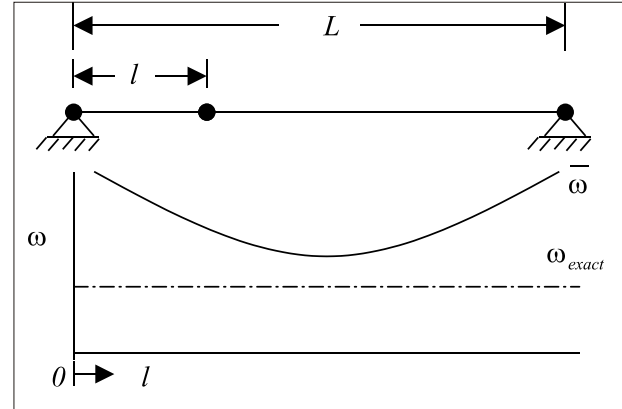

Fig 3.2 The two element moving node sweep test and the variation of natural frequency with respect to the position of the second node

The frequencies obtained as the node is moved are as typically shown in Fig 3.2. If the formulation had been variationally correct, the frequencies would vary in the same convex "egg cup" profile for the Rayleigh-Ritz problem, as the nodal position is moved from a highly asymmetric mesh to a perfectly symmetric mesh. For a uniform beam with symmetric boundary conditions the globally optimal solution would occur when equal length elements are used, i.e. the mid node is placed exactly at the centre of the beam. Interestingly this is also the case where the global errors are equi-partitioned between the two elements. Any other nodal position, as common sense indicates, will be sub-optimal and would produce frequencies with higher errors.

This benchmark will now serve the very useful purpose of examining how this boundedness aspect will suffer if some kind of extra variational relaxation is introduced, either with the formulation of the stiffness matrix, or the mass matrix or both. In this investigation, we will confine attention to changes in the stiffness matrix due to the use of reduced integration. Therefore, a consistent mass matrix is used in all the computations here.

A "sweep test" result for eigenvalues of a thick beam (*L/d=10*) is presented in Fig 3.3 of the shear spectra for locked and lock-free solutions. The locked solution, as it is variationally correct, is upper bound to the exact solution. But as we introduce the "*variational crime*" of reduced integration in the shear energy terms the upper bound nature of the shear spectra is lost.
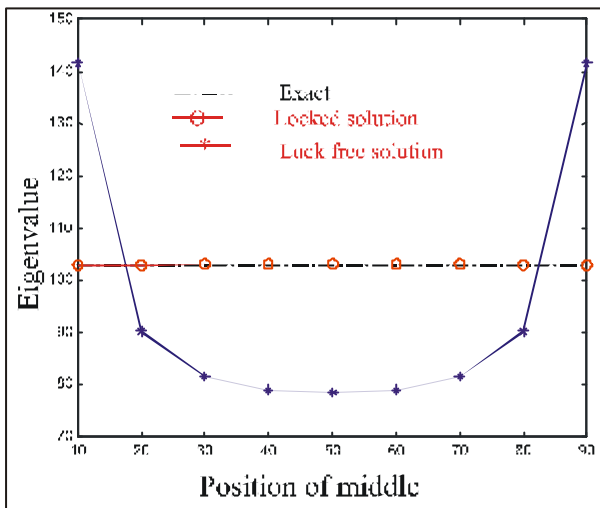
Above experiment confirms that the reduced integration technique is extra variational in nature and produces erroneous results in the shear dominated spectra. Also, it can be noted that for variationally incorrect formulations, the optimisation of eigenvalues by adaptive meshing may give misleading results. For the above example, in the case of reduced integration, the optimum solutions (where the slope of the "egg cup" profile is zero) are not the best solutions; in fact it even predicts the exact solution for a particular position of 2nd node where the error due to mesh distortion compensates for the error due to the variational incorrectness introduced by reduced integration.

P Jafarali, S Mukherjee, G Prathap

3.2 Free vibration analysis of curved beams

Curved beam analysis based on thick arch theory has its differential equation coupled with, axial, bending and shear strains. Hence, the free vibration analysis of the curved beams shows three distinct spectra, each dominated either in axial or in bending or in shear. Hardly any analytical solutions are reported in the literature, even for the simplest case of hinged-roller support conditions, basically due to the complexity of the governing differential equations.
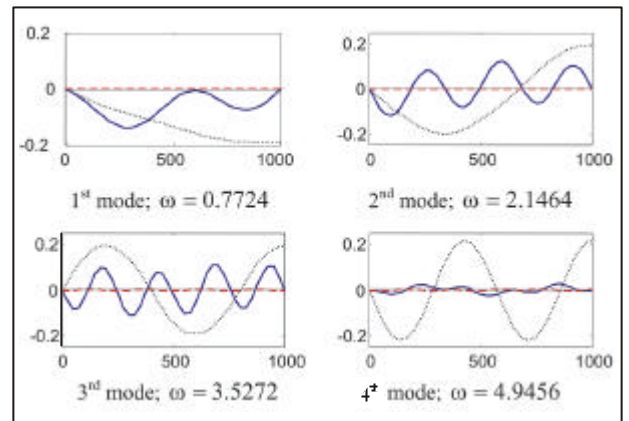

1st mode; $\omega = 0.7724$ 2nd mode; $\omega = 2.1464$

3rd mode; $\omega = 3.5272$ 4th mode; $\omega = 4.9456$

Fig 3.4 First four modes of the axial dominated spectra of a simply supported curved beam (... Axial mode; __ w mode; --- θ mode)

1st mode; $\omega = 0.0546$ 2nd mode; $\omega = 0.2426$

3rd mode; $\omega = 0.5480$ 4th mode; $\omega = 0.9771$

Fig 3.5 First four modes of the flexural dominated spectra of a simply supported curved beam (... Axial mode; __ w mode; --- θ mode)

Pure shear; $\omega = 20.5697$ 1st mode; $\omega = 20.9962$

2nd mode; $\omega = 20.2564$ 3rd mode; $\omega = 20.5697$
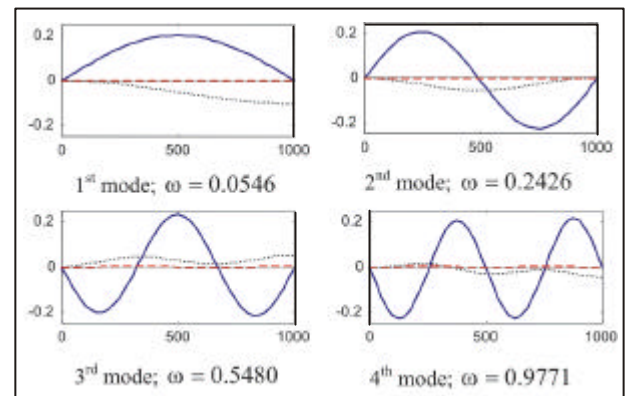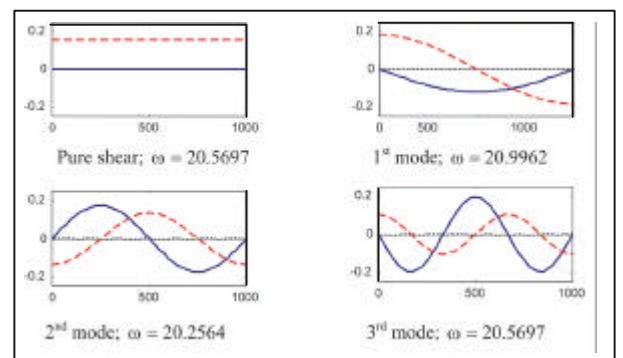
Fig 3.6 First four modes of the shear dominated spectra of a simply supported curved beam (... Axial mode; __ w mode; --- θ mode)

In the present study the in-plane free vibration analysis of a hinged-roller circular arch has been carried out using a two noded shear flexible

curved beam element. The shear flexible curved beam element is very much prone to membrane and shear locking, and for the present analysis these two locking problems have been eliminated using the field consistency approach. The first four mode shapes and the corresponding frequencies of axial, bending and shear spectra are presented in Fig 3.4, 3.5 & 3.6 respectively.

P Jafarali, S Mukherjee , G Prathap

3.3 Error analysis of a hybrid beam element with Timoshenko stiffness and classical mass

Three types of beam elements which are frequently encountered in general purpose packages are critically evaluated from the dynamics point of view. We review critically the performance of an ingeniously designed hybrid beam element that uses a stiffness matrix based on Timoshenko theory but retains the mass matrix from classical beam theory. This clever engineering trick gives seemingly very accurate results in thin beam situations. However, the physics of thick beam behavior is consequently misrepresented. A careful study reveals that cancellation of errors is responsible for the apparent "accurate" performance.

Numerical experiments have been carried out for the calculation of eigenvalues (or frequencies) of free vibration of simply supported beam, for both thin beams (Length to depth ratio, *L/d=100*) and deep beams (*L/d=10*) with *E/kG =2.0*. The hybrid element, which pretends to have the best of both worlds, offers accuracies that lie between that obtained from EB and TB models for thin beam. A careful study shows that seemingly accurate results from this element are due to cancellation of errors, and this has been demonstrated using the two node moving "sweep test" in Fig 3.7. For a deep beam, where comparisons are meaningful only against Timoshenko theory, it becomes obvious that the HB element is not acceptable.

Since this hybrid element uses C^o functions for strain energy and C^1 functions for mass matrix, the effect of rotary inertia of these cross section of the beam is overlooked though the transverse shear deformation is included in the formulation and hence the physics of the problem is
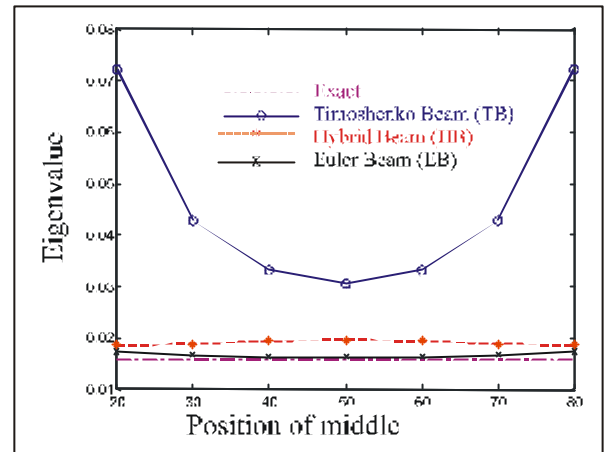

Fig 3.7 Variation of eigenvalues of the flexural spectra with change in position of middle node for a hinged-hinged beam-comparison of finite element EB, TB and HB model (L/d=10)

misrepresented in this element and this aspect is mostly overlooked by unwary production-run analysts. This is obvious from the exercise of investigating the second spectrum and fundamental thickness shear frequency. The HB formulation gives results which are completely at variance with that expected from Timoshenko theory.

P Jafarali, L Chattopadhyay, G Prathap and
S Rajendran

3.4 A priori error analysis of QUAD4 element in elastodynamic problems

The function space approach of a priori error analysis has been well established in finite element literature. However, a priori error analyses in eigenvalue problems are relatively scanty, basically due to the complexity involved in the eigenvalue analysis. Recent investigations in one dimensional finite element elastodynamics using the function space approach were successful in prediction of errors a priori. Prathap and Mukherjee re-derived the projection theorem and the energy-error rule for the finite element elastodynamics using the virtual work principle.

Here, an attempt has been made to extend these predictions for two dimensional free vibration problems. The QUAD4 finite element, based on the Mindlin's plate theory, has been developed and studied extensively using a priori error

analysis. The locking experienced by the QUAD4 element with a rectangular mesh discretisation, has been eliminated using a selective reduced integration for the shear energy, making the element Field-Consistent (FC). It is well known that the Reduced Integration (RI) fails in case of distorted mesh discretisation. It has been also shown earlier for the one dimensional Timoshenko beam elastodynamics that RI is variationally incorrect and will give inaccurate results in the adaptive mesh refinements techniques.

The lock free Edge-Consistent (EC) element originally proposed by Prathap, is amenable to any distorted form of discretisation. The characteristics of this element is being studied for error analysis in elastodynamics.
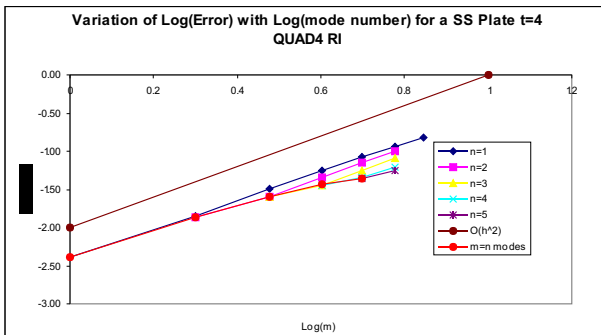

Fig 3.8 Convergence plot for eigenvalues of a thick square plate using QUAD4 RI element

It has been observed from numerical experiments that, for thin plates (L/d=100) the eigenvalues obtained through the QUAD4 RI and the QUAD4 EC elements converge at the order of O(h2) for modes where m = n, and for other modes where m is not equal to n, the eigenvalues converge at a lower rate; this can be attributed to the dominance of twisting effect in these modes.
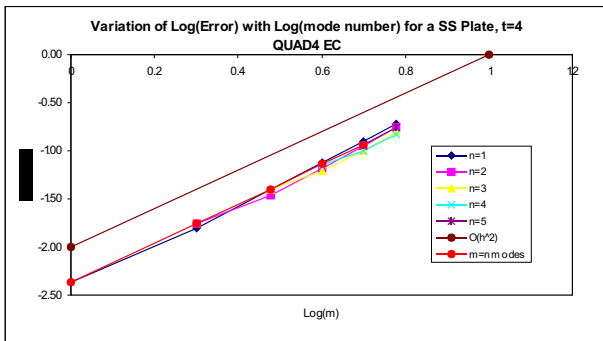

Fig 3.9 Convergence plot for eigenvalues of a thick square plate using QUAD4 EC element.

In the case of thick plate (L/d=10), the QUAD4 RI element does not converge at O(h2). Interestingly the variationally correct QUAD4 EC still converge as predicted from first principles; i.e. at the order of O(h2). This has been presented graphically in Fig 3.8 & 3. 9.

P Jafarali, R Muralikrishna, S Mukherjee and G Prathap

3.5 Analysis of Mindlin plate element from the function space approach

Despite satisfying completeness and continuity requirements isoparametric elements with multiple strain components are prone to suffer spurious stiffness properties and corresponding stress oscillations. This kind of error, commonly known as Locking is generally circumvented through reduced integration techniques applied to evaluate the element stiffness matrices. Using the field consistency paradigm one can view this technique as a means to suppress spurious, field-inconsistent terms in the strain energy of the element. Recently, the function space approach has been used to explain the origin and elimination of locking in simple Timoshenko beam elements. This approach substantiates the postulates of the field consistency paradigm. The objective of this work is to unify the arguments from function space approach and field-consistency method to address locking in Mindlin-Plate element.

Mindlin plate elements account for bending deformation and for transverse shear deformation so that the stiffness matrix $[k]$ can be regarded as being composed of a bending stiffness $[k_b]$ and a transverse shear stiffness $[k_s]$. Locking of Mindlin plate elements caused by too many transverse shear constraints can be avoided by adopting a reduced or selective integration rule to generate $[k]$.

The 4-noded bilinear element is the simplest element based on Mindlin theory. It was established that, a fully integrated bilinear element even in its rectangular form would lock when used to analyze thin plates. Locking was seen to vanish if a 2x2 Gauss rule was used to

Evaluate $[k_b]$ and a reduced 1-point rule was used to evaluate $[k_s]$. An analysis of the element from

the function space approach revealed a loss in dimension of the space spanned by the column vectors of the B matrix arising from the strain - displacement relationship. This deficiency was attributed to the zero energy mechanisms of the bilinear element arising with reduced integration.

Table 3.1 Comparision of element mechanisims and the loss of dimension of B space for various integrations order

Element Type	Integration Rule			No. of Mechanisms	Dimension of B space
	Type	$[k_b]$	$[k_s]$		
Four noded (12 d.o.f)	Reduced	1x1	1x1	4	5
	Selective	2x2	1x1	2	7
	Shear Selective	2x2	2x1 1x2	0	9
	Full	2x2	2x2	0	9

As shown in the Table 3.1. Full integration is sufficient to avoid element mechanisms, but causes locking. A 1-point integration of the bending and stiffness matrices eliminates locking but has 4 additional mechanisms. This is also revealed by the loss in dimension of the solution space (from 9 to 5) spanned by the column vectors of the B-matrix. A selective integration of the bending and stiffness matrix also eliminates locking but brings in two mechanisms in addition to the usual three rigid body modes that may lead to the deterioration of the element performance. Thus both reduced and selective quadrature rules failed to eliminate locking without introducing other deficiencies. An optimal integration strategy suggested by the field consistency method is to use a 2x2 Gauss rule to evaluate $[k_b]$, a 1x2 Gauss rule to evaluate γ_{yz} and a 2x1 Gauss rule to evaluate γ_{yz}. An analysis of this element from function space approach reveals no reduction in the dimension of the space spanned by the column vectors of the B-matrix. This suggests that the field consistency arguments lead to optimal integration strategies without introducing any zero energy mechanisms. This element would be the optimal rectangular bilinear element. This also suggests that knowledge of the dimension of the solution space spanned by the column vectors of B can be helpful in choosing an optimal integration strategy to get a lock free element.

K Sangeeta, S Mukherjee and G Prathap,

3.6 Free vibration analysis of composite beams using higher order shear deformation theory

A finite element model using C^0 continuity is developed to analyse the natural frequencies and the mode shapes of the laminated composite beam using LCW shear deformation theory.The finite element model consists of a two noded Timoshenko beam element.The present element has seven degrees of freedom per node. The classical EulerBernoulli theory assumes that the transverse normal to the neutral axis remains same during bending and after bending. It indicates that the transverse shear strain is zero. In the case of laminated composite beams, this theory fails to predict the behavior of the structures accurately. The advantage of the LCW theory over the first order shear deformation theory (FSDT) is that the first order theory assumes transverse shear strain distribution is assumed to be constant through the beam thickness and thus the FSDT requires a shear correction factor. But in the case of LCW theory, the shear correction factor is not required.

A program is developed in MATLAB platform to obtain the natural frequencies and mode shapes.The natural frequencies and mode shapes of laminated cross-ply composite beams are studied. In the present study, the locked solution (exact integration) and the lock-free solution (reduced integration) are studied for various boundary conditions and compared with exact solution.

G Prathap and V Senthilkumar

3. 6 The motion of periodically forced spheroids in simple shear flow

The work initiated by the author at RRL - Trivandrum on the dynamics and rheology of periodically forced spheroids in simple shear flow has been continued. There are certain intrinsic factors to this problem which appear to give it greater significance than appears at first sight. 1). This problem is physically accessible to suitable experiments. 2) This system is an example of a system in which a periodic forcing of the individual spheroids is related to a periodic forcing of the collective behaviour of appropriate averages over the orientations of individual spheroids
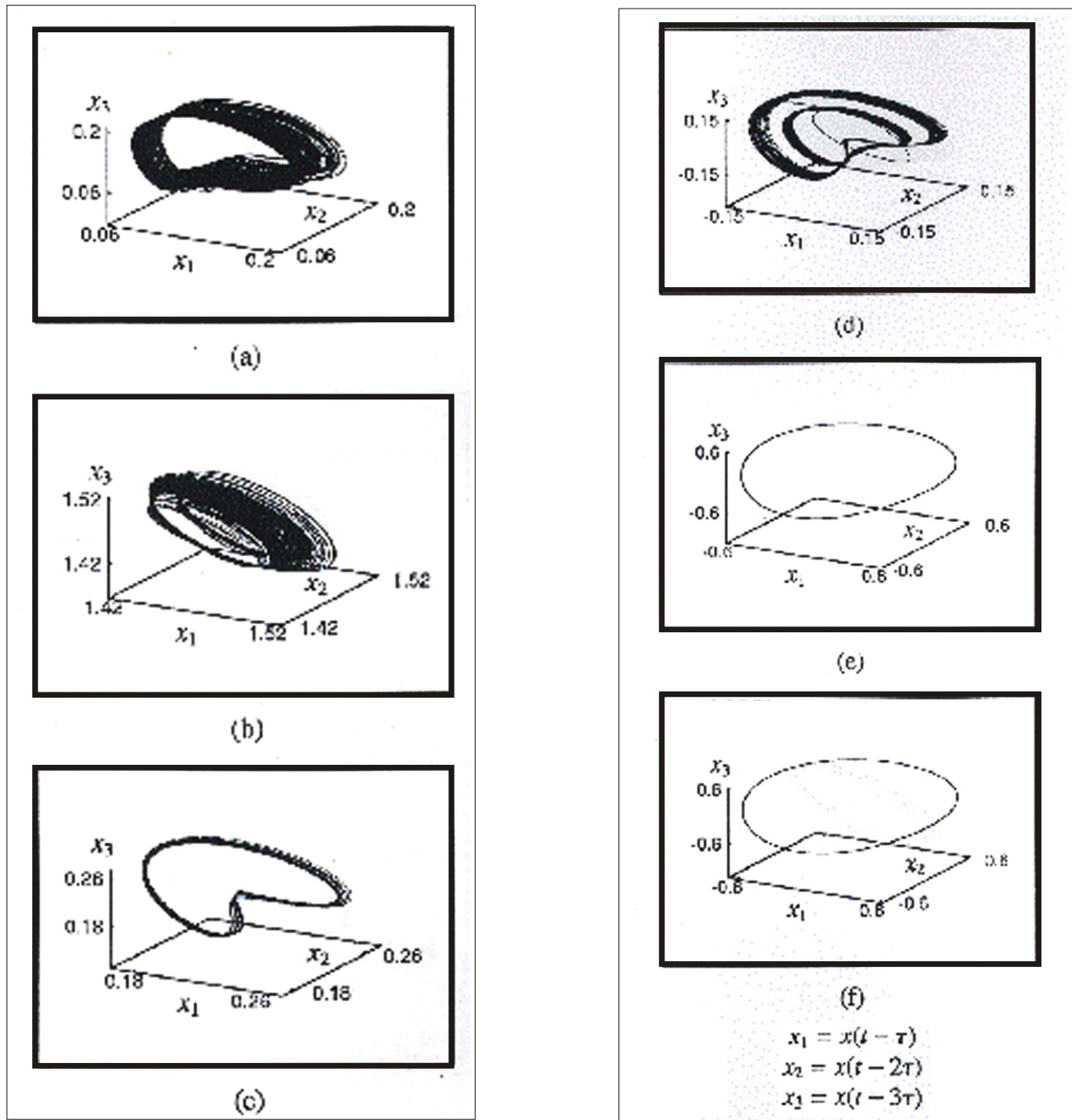
Fig. 3.10 Three dimensional embedding of the attractors reconstructed from the time series of the apparent viscosity and the first normal stress difference for various values of Pe (a measure of the strength of the Brownian force to the viscous force). (a) & (d) Pe =0.0; (b) & (e) Pe=0.01; (c) & (f) Pe=0.1 showing a quasiperiodic transition to chaos as Pe decreases.

$$x_1 = x(t - \tau)$$
$$x_2 = x(t - 2\tau)$$
$$x_3 = x(t - 3\tau)$$

through a common periodic forcing term. It appears, thus that this system can be considered to be an idealized version of a general system which appears to be relatively common in which one is interested in the periodically forced average behaviour of a large number of individually periodically forced particles. During the present year the analysis has been extended to the case of periodically forced Brownian particles using the technique developed by Asokan   et al.. We have observed chaos in the normal stresses and the apparent viscosities and a quasiperiodic route to chaos as shown in Fig.3.10 for the first normal stress difference and

the apparent viscosity. We note that as the relative strength of the Brownian force to the shear force increases, the system behaviour becomes regular. The details of the investigation are reported in Asokan and Ramamohan. We are currently preparing a review of the results of our work in this area since 1994.

K Asokan , T R Ramamohan

3.7 Isotropic Numerical Schemes

Conventional numerical schemes are directionally biased. New finite-differences, called isotropic finite-differences have been developed. Some application of numerical schemes based on these finite-differences are shown.
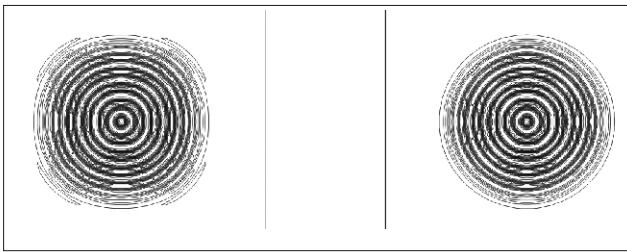

Fig 3 .11 A comparison of solutions of Cahn-Hilliard equation obtained using (a) Conventional scheme, and (b) isotropic scheme on a 100 X 100 grid with *h* = 0:01.

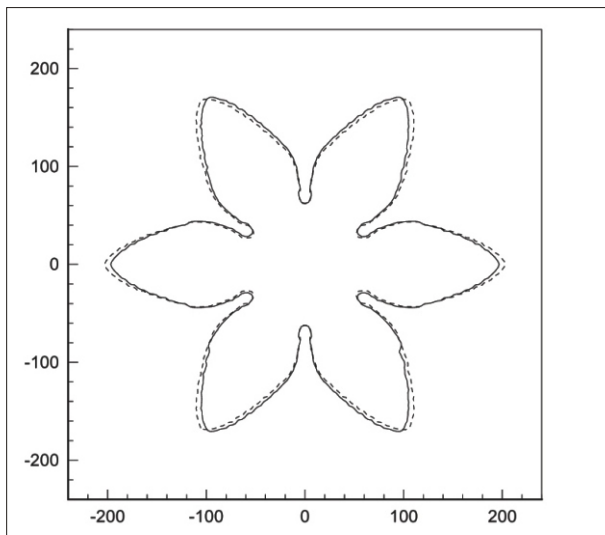Fig. 3.11 shows a simulation of Cahn-Hilliard equation governing phase separation in bimetallic

Fig 3.12 A comparison of the solidfication fronts obtained using the isotropic scheme, -----, and the conventional scheme, - - - - -. t = 400.

mixture due to quenching from a single point. The physics requires that phase pattern be symmetric, i.e. circular in two dimension. However simulation by a conventional scheme does not give the symmetric pattern. The problem is one of anisotropy in the conventional scheme. Using isotropic scheme the symmetric pattern is easily obtained. This has great consequences on a general simulation. Experimentally possible phase pattern may never be obtained using conventional scheme.

Fig. 3.12 shows a simulation of dendritic solidification. We have considered a six-fold dendritic solidification, and look for the six-fold symmetric pattern in the simulation. It is found that while the symmetry is well preserved in the simulation using the isotropic scheme, it is poorly captured in the simulation using the conventional scheme.

A Kumar

3.8 The Quasi-Equilibrium Phase in Purely Nonlinear Chains with Boundaries

The study of normal modes in $1D$ mass-spring systems is central to our understanding of basic lattice dynamics starting from the initiation of a velocity perturbation imparted at a site to the distribution of the perturbation energy among the available modes of the system, i.e., of the *equipartitioning* of the available energy. Chains with combined harmonic and anharmonic springs have attracted significant attention since 1950s starting with the celebrated Fermi-Pasta-Ulam (FPU) problem. The study of the dynamics of such nonlinear chains has precipitated fundamental advances in our understanding of solitons and have led us to examine issues such as the equipartitioning of perturbation energy into available modes of the system and of the approach to equilibrium in systems with highly nonlinear interactions.

In this work, we focus on systems which have no harmonic term in the interaction potential at all - meaning systems in which the masses do not necessarily move back and forth in *rhythmic harmonic motion* to produce phonons or sound waves. An example is that of repulsion between two elastic grains upon compression, which is completely nonlinear. Any perturbation in such

systems, irrespective of its magnitude, travels as shock waves (typically as a single large shock wave followed by many tiny ones). It is conceivable that some long chain biological molecules (such as proteins) may exhibit strongly nonlinear interactions albeit with a weak harmonic part to the interaction.

We consider systems placed between rigid (or for that matter soft) boundaries as well as systems with periodic boundary conditions. The presence of boundaries is best viewed as a way to alter the local conditions associated with the travel of some perturbation in the systems of interest and leads to significant modifications in the system dynamics. We keep our focus on perturbations initiated by setting some velocity or velocities to non-vanishing values at the initial instant. We do not consider perturbations initiated only by stretching bonds, which may give rise to long-lived localized modes (intrinsic localized modes ILMs).

We start by considering a Hamiltonian of the following form,

$$E= \sum_{i=1}^{N} \frac{p^2}{2m} + \alpha_1 \sum_{i=1}^{N} V_1(x_{i,i+1}^2) + \alpha_2 \sum_{i=1}^{N} V_2(x_{i,i+1}^{\beta}), \ \beta>2 \quad (3.3)$$

Where v_1 is the harmonic term and v_2 is the anharmonic term. We consider our chain systems to be finite, typically with N between 20 and 100. The systems satisfy periodic boundary conditions or are placed between rigid walls.

The parabolic potential introduced by the v_1 term allows the particles in the 1D chain to move back and forth about their equilibrium positions with any of the allowed harmonic frequenci*es* of the system and thus *share* their energies with other masses in the system. Given that >2, the anharmonic potential, v_2, is *softer* than harmonic when the masses are slightly pushed into one another but *steeper* than harmonic when two adjacent particles get sufficiently close. Thus, when a particle starts closing in on a neighbor, initially the dynamics is slow, and then as the potential steepens, the rapidly developing repulsion gets the particles to abruptly recoil. The energy transfer during such processes is inevitably in a "bundled" form and unlike the harmonic case, there is less oscillation of the particles due to v_2 . Bundled

energy transfer is often associated with the presence of solitary waves and of solitary wave-like objects in systems.

When both V_1 and V_2 are present in a system, the harmonic term allows extended oscillations and thus facilitates the sharing of modes between particles, in addition to supporting the presence of solitary waves. Our simulations suggest that the presence of V_1 tends to drive the system to a state with equipartitioned energy at asymptotically large times.

When $_1 = 0$, a system only transfers energy from one mass to the next via solitary waves. The solitary waves are always of fixed spatial width. This spatial width is controlled by . When , the width of the solitary wave shrinks to the minimum physically meaningful width. The solitary waves that end up running through a bounded system continuously collide with each other. Unlike solitons, solitary waves may not necessarily preserve themselves upon collision with another solitary wave. The collision process in our system is such that the waves end up leaving tiny residual solitary waves after a collision event and attenuates slightly in amplitude through the collision process. Eventually, the system drives itself into a state in which a large set of small amplitude solitary waves of various amplitude distributions and speeds are found in the process of constant modication as they collide. The perturbation energy is never equipartitioned in these systems and the systems forever remain in the "quasi-equilibrium" state, which is necessarily characterized by large fluctuations against what would have been the fluctuations in a state with energy equipartitioning. Our simulations suggest that the final state of the system is independent of initial velocity perturbation conditions (e.g., whether the velocity perturbation was imparted to one particle at a desired position or to two chosen particles or more, etc.).

In Fig 3.13, we present a description of the emergen3.16e of this equilibrium-like phase. In Fig 3.13(a), the data suggest that the average velocity of the particles remain time dependent at all times. in Fig. 3.13(b), we show that the velocity distribution of the particles is Gaussian and, in Fig. 3.13(c), we show that the velocity power spectrum of a typical particle decays logarithmically in frequency in the nonlinear system, in contrast to
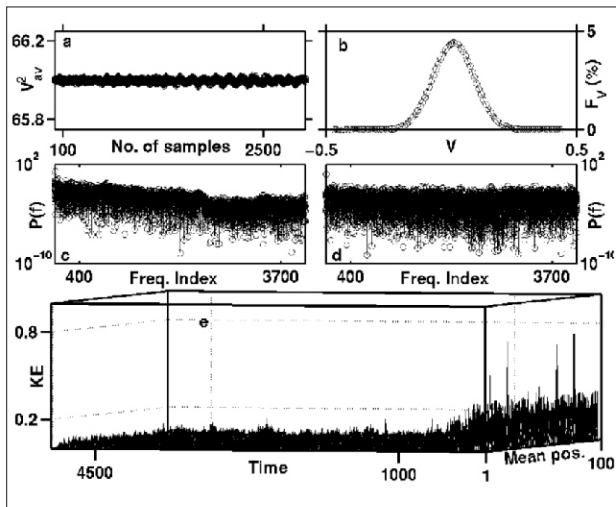
Fig 3.13 Nature of asymptotic state. The first panel (Figs. 3.13(a)) shows the spatial average of v^2, which is again averaged over a time period $T = 3000$; 3000 samples each are shown, which have been taken from consecutive starting points, after 75000 time steps of integration. Onefinds bigger fluctuations for averages over $T < 3000$. Fig 3.13(b) shows that the velocity distribution of the particles is Gaussian in the quasi-equilibrium state. Fig.3.13(c) and Fig.3.16(d) present the velocity power spectrum of the 25th particle in the system for the purely quartic and the purely harmonic systems, respectively. Both panels are for periodic boundary conditions. The FFT is similar if it is taken over the maximum velocity in the chain at successive instants. Fig 1.13(e) shows the kinetic energy of each particle against time; the data conveys the rapidity with which the quasi-equilibrium phase is reached.

remaining roughly flat in harmonic systems, which is shown in Fig 3.13(d). The power spectrum of the maximum velocity of the particles also follows the behavior shown in Fig 3.13 (c)-(d). It may be noted that as system size grows, progressively small amplitude solitary waves are readily allowed in the system. Hence, one would expect that the log logarithmic slope of the velocity power spectrum will become progressively flat. Indeed, this is what is found in preliminary studies to be reported elsewhere. In the limit of particle number going to   , the dierences between the quasi-equilibrium state and the equipartitioned state become essentially indistinguishable.

T R Krishna Mohan and Surajit Sen